



# Wave reflection quantification based on pressure waveforms alone—Methods, comparison, and clinical covariates

Bernhard Hametner<sup>a,b,1</sup>, Siegfried Wassertheurer<sup>a,b,\*,1</sup>, Johannes Kropf<sup>a</sup>,  
Christopher Mayer<sup>a</sup>, Andreas Holzinger<sup>c</sup>, Bernd Eber<sup>d</sup>, Thomas Weber<sup>d</sup>

<sup>a</sup> Health & Environment Department, AIT Austrian Institute of Technology, Vienna, Austria

<sup>b</sup> Department of Analysis and Scientific Computing, Vienna University of Technology, Vienna, Austria

<sup>c</sup> Institute of Medical Informatics, Medical University Graz, Austria

<sup>d</sup> Cardiology Department, Klinikum Wels-Grieskirchen, Wels, Austria

## ARTICLE INFO

### Article history:

Received 26 January 2012

Received in revised form

12 September 2012

Accepted 4 October 2012

### Keywords:

Wave separation analysis

Arterial stiffness

Reflection magnitude

Augmentation pressure

Augmentation index

## ABSTRACT

Within the last decade the quantification of pulse wave reflections mainly focused on measures of central aortic systolic pressure and its augmentation through reflections based on pulse wave analysis (PWA). A complementary approach is the wave separation analysis (WSA), which quantifies the total amount of arterial wave reflection considering both aortic pulse and flow waves. The aim of this work is the introduction and comparison of aortic blood flow models for WSA assessment. To evaluate the performance of the proposed modeling approaches (Windkessel, triangular and averaged flow), comparisons against Doppler measurements are made for 148 patients with preserved ejection fraction. Stepwise regression analysis between WSA and PWA parameters are performed to provide determinants of methodological differences. Against Doppler measurement mean difference and standard deviation of the amplitudes of the decomposed forward and backward pressure waves are comparable for Windkessel and averaged flow models. Stepwise regression analysis shows similar determinants between Doppler and Windkessel model only. The results indicate that the Windkessel method provides accurate estimates of wave reflection in subjects with preserved ejection fraction. The comparison with waveforms derived from Doppler ultrasound as well as recently proposed simple triangular and averaged flow waves showed that this approach may reduce variability and provide realistic results.

© 2012 Elsevier Ireland Ltd. All rights reserved.

## 1. Introduction

Arterial stiffness and its clinical surrogates determined by pulse wave analysis (PWA) and pulse wave velocity (PWV) became emerging concepts in cardiovascular risk stratification [1–4] recently. The quantification of increasing pulse wave reflections, due to increased arterial aging and pathological

changes along the arterial tree, mainly focused on measures of central aortic systolic pressure (aSBP), augmentation index (AIx), and augmentation pressure (AP) as illustrated in Fig. 1A. These methods utilize time domain analysis and are applied to pressure signals only [5,6]. Various investigators demonstrated that both elevated aSBP and AIx are independent predictors of cardiovascular risk [7], morbidity and mortality in patients with end stage renal disease [8,9] and coronary heart disease

\* Corresponding author at: Health & Environment Department, AIT Austrian Institute of Technology GmbH, Viktor Kaplan Straße 2/1, 2700 Wiener Neustadt, Austria. Tel.: +43 50550 4830; fax: +43 50550 4840.

E-mail addresses: [Siegfried.Wassertheurer@ait.ac.at](mailto:Siegfried.Wassertheurer@ait.ac.at), [Bernhard.Hametner@ait.ac.at](mailto:Bernhard.Hametner@ait.ac.at) (S. Wassertheurer).

<sup>1</sup> These two authors contributed equally to this work.

0169-2607/\$ – see front matter © 2012 Elsevier Ireland Ltd. All rights reserved.

<http://dx.doi.org/10.1016/j.cmpb.2012.10.005>

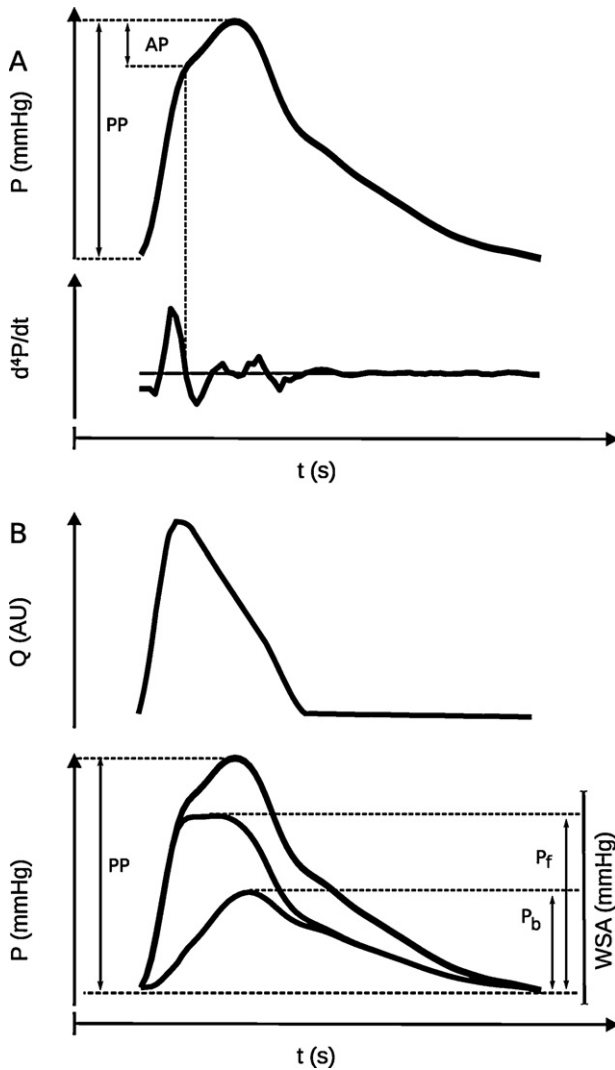


**Fig. 1 – (A) Pulse wave analysis: augmentation pressure (AP) determination based on higher order derivatives of pressure wave alone. (B) Aortic flow wave acquired by Echo is used to decompose aortic pressure wave with wave separation analysis method (please note that there is a difference in paradigm between PWA and WSA and therefore PP is not equal to  $P_f + P_b$ ).**

[10–13]. Furthermore it was reported that the Alx correlates with the left ventricular mass in normotensive men as well as in hypertensive ones [14]. Moreover, the increase in cardiovascular risk can be estimated better from central than from brachial blood pressure measurements [1,9,15].

A complimentary approach and measure of wave reflection is known as wave separation analysis (WSA). Based on previous findings in animals and humans [16,17] this method has been proposed by Westerhof et al. in 1972 by introducing a frequency domain method to quantify the total amount of arterial wave reflection considering both aortic pulse and flow waves [18] (Fig. 1B). However, the assessment of ventricular flow in routine is laborious and the shape and magnitude of flow waves may get changed by aging, ventricular function or cardiovascular pathology [19–21]. To overcome the obvious

difficulties in the non-invasive assessment of aortic flow and with focus on subjects without heart failure recently a set of papers were published discussing simplified approximations of aortic flow to calculate wave reflection and its measures [22–27].

Indeed based on this work but using the very simplified triangular flow model Wang et al. [28] recently reported a 15 year community based longitudinal study which confirmed for the first time that the total amount of arterial wave reflection predicts long-term cardiovascular mortality in men and women independent of arterial stiffness. Recently presented own follow up data on 725 patients with preserved ejection fraction [29] provide, similar to Wang et al., evidence that WSA parameters of wave reflection may be more closely related to cardiovascular target organ damage and endpoints than measures of PWA.

The aim of this work is the introduction of an aortic blood flow model based on higher order Windkessel theory (ARCSolver), its comparison against conventional Doppler Echocardiography-based WSA, and other models found in the literature, as well as the determination of their relationship to more conventional measures of arterial wave reflections (PWA) in a study cohort with preserved ejection fraction.

## 2. Materials and methods

### 2.1. Study population

Overall 148 patients with suspected coronary artery disease (CAD) have been included in the study, 120 males and 28 females. Exclusion criteria were rhythm other than stable sinus rhythm, impaired systolic function, valvular heart disease, and unstable clinical presentation. Medications were not withheld throughout the study. The measurements were carried out at the Department of Cardiology in the University Teaching Hospital of Wels-Grieskirchen in Wels, Austria. They were performed within the framework of various ongoing projects, authorized by the regional ethics committee and patients gave written informed consent.

### 2.2. Data assessment

Assessment procedures were applied as proposed by Segers et al. [30]. The arterial flow velocity waveforms were measured by Doppler ultrasound in the apical 5-chamber view at the level of the left ventricular outflow tract over several heartbeats using a Philips iE33 ultrasound machine. Thereafter the waveforms were manually digitalized. To assess aortic pressure waveforms as well as augmentation pressure, radial artery waveforms were recorded using a Millar SPT 301 tonometer and the corresponding synthesized aortic waveforms and all PWA parameters were calculated using the validated SphygmoCor system (AtCor Medical Pty. Ltd., West Ryde, Australia). For Doppler WSA pressure and flow curves were carefully aligned in time using visual characteristics, i.e. aligning the onset of flow to the steep rise of the early systolic pressure curve and the diastolic notch of the pressure curve to the cessation of flow.

Brachial blood pressure was measured in the supine position with a validated automated oscillometric device (Omron Hem 757, Omron Corporation, Kyoto, Japan).

### 2.3. Triangular and average waveform construction

The simplest way to estimate the flow is to use a triangular waveform, as proposed previously [23,24]. The starting point of the triangle is assigned to the onset of the corresponding pressure curve, which marks the beginning of the pressure upstroke during systole. The maximum of the triangle is set to the moment of time ( $t_{Q_{max}}$ ) when the inflection point of the pressure wave is detected. The maximum slope of the flow wave ( $dQ_{max}$ ) therefore obviously depends on  $t_{Q_{max}}$ . Another approach was proposed by Kips et al. [22], they used an averaged waveform based on 74 samples. The averaged waveform is mathematically described as a Fourier-series and published for the first 10 harmonics. Scaled from 0 to 100 arbitrary units (AU), both curves are interpolating the systolic time interval heart rate dependent and are finally set to zero in the diastolic period.

### 2.4. Windkessel (ARCSolver) waveform construction and wave separation analysis

Windkessel (WK) models are well established to estimate arterial properties [31]. Our method describes the outflow of the left ventricle ( $Q_m$ ) during systole based on an externally (in this study by SphygmoCor) provided central pressure waveform ( $P_m$ ) similar to an 3-element Windkessel model by the means of a dynamic system of second order. Unlike the approach used by Wesseling et al. [25] who introduced a non-linear model with tabulated values for vascular properties, we propose a linear model with continuous parameter space for arterial resistance ( $R_C$ ), peripheral resistance ( $R_p$ ) and arterial compliance ( $C_a$ ). A fully mathematical description is given in the appendix but to summarize the three steps: (1) the equations for  $R_C$ ,  $R_p$  and  $C_a$ , are supposed to be formulated as an isoperimetric problem with a constraint to minimize external work. Calculus of variation and application of Lagrange formalism results in a linear inhomogeneous second order system, which can be solved adequately [32–35]. Numerical parameter values for  $R_C$ ,  $R_p$  and  $C_a$  are then obtained by the method of pressure waveform area fitting using the Levenberg–Marquardt method (Fig. 2A and B). (2) In an additional step the so calculated Windkessel flow is processed using a second order linear delay element to get the final flow wave shape (Fig. 2C). This particular delay element is mainly characterized by two individual dependent time constants ( $T_1$ ,  $T_2$ ) and an intermediate buffer variable ( $b$ ). (3) Transmission line theory, which is described in the next paragraph, is applied to these waveforms to assess wave reflection.

To perform the separation, three variables are needed: The measured pressure ( $P_m$ ) and modeled flow ( $Q_m$ ) wave in the aorta and furthermore the characteristic impedance ( $Z_c$ ), which represents the impact of the arterial wall and therefore the relation between pressure and flow.  $Z_c$  is estimated in the frequency domain using the modulus of the complex input impedance ( $Z_i$ ) calculated from the ratio of the present pressure and flow in the frequency domain. The

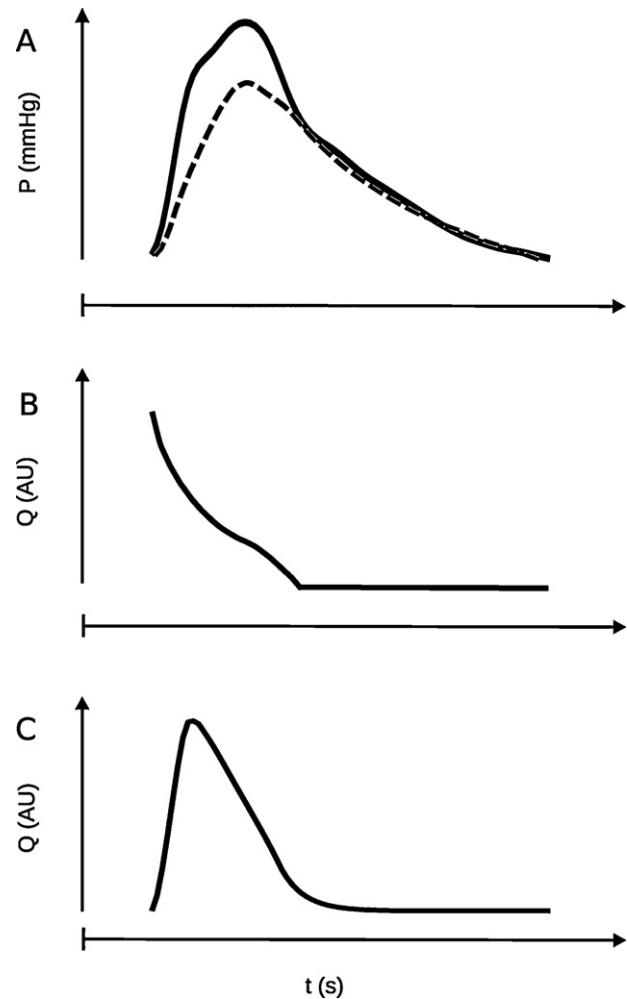


**Fig. 2 – (A) Central pressure waveform (solid) and fitted Windkessel pressure waveform (dotted). (B) Windkessel flow derived from ApEqs. (1) and (2). (C) Realistic flow pattern provided by ARCSolver after ApEq. (15) has been applied to Windkessel flow.**

frequencies in the range of 4–10 Hz are taken into account, which is a commonly used procedure [18,22,23,36]. For higher frequencies there could be inaccuracy due to noise [21]. To minimize the influence of outliers, all input impedances greater than a factor of 3 of the median of the considered harmonic waves are not taken into account [30]. Following the wave theory, the measurable pressure ( $P_m$ ) in the aorta is the sum of forward ( $P_f$ ) and backward ( $P_b$ ) traveling waves [18]. The same is valid for the corresponding flow waves. To obtain the forward and backward going parts separately, these equations have to be transformed ( $P_f = 0.5 \times [P_m + Z_c \times Q_m]$  and  $P_b = 0.5 \times [P_m - Z_c \times Q_m]$ ), in order to obtain explicit formulas for the requested parameters (see also Fig. 1C). It should be noted that the absolute amplitude of  $Q_m$  is not relevant for the decomposition. If  $Q_m$  is changed by a certain factor, the resulting characteristic impedance will be altered by the same factor in an inverse manner. Thus the calculated waves in forward and backward direction remain unchanged. Based on forward and backward pressure amplitudes, two parameters can be

derived, the reflection magnitude (RM) and the reflection index (RI). The reflection magnitude is the quotient of the backward and forward amplitude of the separated pressure waves. For the reflection index the denominator is changed to the sum of the two amplitudes.

2.5. Statistical analysis

All measurements are given as mean and standard deviation (SD). Pairwise measured differences are analyzed by mean difference, standard deviation as well as 95% confidence interval for the mean. Limits of agreement and residual distribution are presented using Bland–Altman plots. Regression coefficients are also stated with their 95% confidence intervals. Wave shapes are compared using the root mean square error (RMSE), which is the generalized analog of the mean standard error but for data following an unknown distribution and ANOVA. In order to compare the flow curves that are generated in different ways properly, they are normalized to 100 arbitrary units (AU). The reason to use arbitrary units is due to modeling properties in the triangular and averaged waveform approach. There is a comprehensive discussion in Westerhof et al. [24] why this approach is consistent and useful. Although AP and  $P_b$  are both measures of reflected waves their particular predictive value on outcome may be method dependent [28,29]. Stepwise regression analysis is applied to assess clinical covariate(s) and their contribution at each marker level. For the analysis the statistical software of Matlab version 2009b (The Mathworks Inc., Natick, USA) is used.

3. Results

3.1. Study population

The mean age was 60.3 years (SD 12.1 years). The lower age limit was 18 years, the upper one 81 years. The mean

**Table 1 – Baseline clinical data (SBP = systolic blood pressure, DBP = diastolic blood pressure,  $R_p$  = peripheral resistance,  $C_a$  = arterial compliance,  $T_1$  and  $T_2$  = index based time constants,  $b$  = intermediate flow state variable,  $Z_c$  = characteristic impedance).**

Men/women	120/28
Age (years)	60.3 (12.1 SD)
Weight (kg)	84.6 (15.1 SD)
Height (cm)	172.5 (9.3 SD)
Hypertension	105 (70.9%)
Diabetes	27 (18.2%)
Smoker	28 (18.9%)
Coronary artery disease	57 (38.5%)
Heart rate (1/min)	64 (10 SD)
SBP peripheral (mmHg)	131 (17 SD)
DBP peripheral (mmHg)	81 (9 SD)
SBP central (mmHg)	121 (16.0 SD)
DBP central (mmHg)	82 (10 SD)
$R_p$ (mmHg*s/ml)	1.41 (0.18 SD)
$C_a$ (ml/mmHg)	0.90 (0.28 SD)
$T_1$	4.39 (0.55 SD)
$T_2$	1.10 (0.02 SD)
$b$ (AU)	57.8 (6.6 SD)
$Z_c$ (AU)	0.20 (0.07 SD)

peripheral systolic blood pressure was 131 mmHg (SD 17 mmHg), the mean peripheral diastolic blood pressure was 81 mmHg (SD 9 mmHg). More information on the basic clinical data is shown in Table 1.

3.2. Comparison of flow curves

The average timing of the flow curve maximum ( $t_{Q_{max}}$ ) for the measured (Doppler derived) flow is 0.084 (0.008 SD)s, for the triangular flow 0.107 (0.013 SD)s, for the averaged flow 0.085 (0.007 SD)s and for the WK flow 0.088 (0.006 SD)s To determine the shape of the different flow curves, the maximal slope ( $dQ_{max}$ ) can serve as an indicator. For the measured flow the mean maximal slope is 1491 (227 SD) AU, for the triangular flow

**Table 2 – Aggregated values and pairwise comparison of parameters derived from each introduced flow approximation approach (est = estimated) vs parameters derived from Echo (Doppler). Values in brackets are 95% confidence intervals for differences and correlation coefficients (R = Pearson’s correlation coefficient,  $P_f$  = forward pressure wave amplitude,  $P_b$  = backward pressure wave amplitude,  $P_m$  = aggregated pressure wave,  $Q_m$  = flow wave,  $t_{Q_{max}}$  = timing of maximum flow,  $dQ_{max}$  = maximum slope of flow, RM = reflection magnitude, RI = reflection index).**

	Echo	WK	Triangular	Average
$t_{Q_{max}}$ (s)	0.084 (0.008 SD)	0.088 (0.006 SD)	0.107 (0.013 SD)	0.085 (0.007 SD)
$dQ_{max}$ (AU)	1491 (227 SD)	1646 (131 SD)	948 (100 SD)	3078 (226 SD)
RMSE [( $Q_m$ ) <sup>est</sup> – ( $Q_m$ ) <sup>echo</sup> ] (AU)	–	4.68 (1.90 SD)	6.12 (2.33 SD)	8.08 (1.09 SD)
$P_f$ (mmHg)	26.56 (7.96 SD)	26.17 (7.54 SD)	33.21 (10.78 SD)	26.11 (8.08)
$P_b$ (mmHg)	16.66 (5.46 SD)	15.64 (5.47 SD)	18.67 (7.34 SD)	18.72 (5.74 SD)
RMSE [( $P_f$ ) <sup>est</sup> – ( $P_m$ ) <sup>echo</sup> ] (mmHg)	–	0.82 (0.54 SD)	2.34 (1.57 SD)	0.93 (0.41 SD)
( $P_f$ ) <sup>est</sup> – ( $P_f$ ) <sup>echo</sup> (mmHg)	–	–0.39 (1.96 SD)	6.66 (4.67 SD)	–0.45 (1.71 SD)
		[–0.71 –0.07]	[5.89 7.43]	[–0.73 –0.17]
R [( $P_f$ ) <sup>est</sup> vs ( $P_f$ ) <sup>echo</sup> ]		0.970	0.919	0.977
		[0.959 0.978]	[0.890 0.941]	[0.968 0.983]
( $P_b$ ) <sup>est</sup> – ( $P_b$ ) <sup>echo</sup> (mmHg)	–	–1.02 (1.31 SD)	2.01 (3.87 SD)	2.06 (1.19 SD)
		[–1.24 –0.80]	[1.37 2.65]	[1.86 2.26]
R [( $P_b$ ) <sup>est</sup> vs ( $P_b$ ) <sup>echo</sup> ]	–	0.971	0.858	0.979
		[0.960 0.979]	[0.809 0.895]	[0.971 0.985]
RM	0.63 (0.10 SD)	0.59 (0.09 SD)	0.56 (0.09 SD)	0.72 (0.07 SD)
RI	0.38 (0.04 SD)	0.37 (0.04 SD)	0.36 (0.04 SD)	0.42 (0.02 SD)

948 (100 SD) AU, for the averaged flow 3078 (226 SD) AU and for the WK flow 1646 (131 SD) AU. With the root mean square error (RMSE), the deviation of two curves based on the difference for each data point can be measured. The mean RMSE between the measured flow and the triangular flow curve is 6.12 (2.33 SD) AU, the mean RMSE between the measured flow and the averaged flow is 8.08 (1.09 SD) AU and the mean RMSE between the measured flow and the WK flow is 4.68 (1.90 SD) AU for a peak flow of 100 arbitrary units, and these RMSE are significantly different ( $P < 0.05$  in ANOVA). Table 2 provides a summary of the main results.

### 3.3. Comparison of wave separation parameters

For the forward pressure wave ( $P_f$ ), the mean amplitude calculated from the measured Doppler flow is 26.56 (7.96 SD) mmHg, taking the triangular flow 33.21 (10.78 SD) mmHg, using the averaged flow 26.11 (8.08 SD) mmHg and with the WK flow 26.17 (7.54 SD) mmHg. For the backward pressure wave ( $P_b$ ), the mean amplitude calculated from the measured Doppler flow is 16.66 (5.46 SD) mmHg, taking the triangular flow 18.67 (7.34 SD) mmHg, using the averaged flow 18.72 (5.74 SD) mmHg and with the WK flow 15.64 (5.47 SD) mmHg. Subsequently the mean differences for WK derived amplitudes against Doppler derived ones are  $-0.39$  (1.96 SD)  $[-0.71|-0.07]$  mmHg and  $-1.02$  (1.31 SD)  $[-1.24|-0.80]$  mmHg for the amplitudes of  $P_f$  and  $P_b$ , respectively. Bland Altman plots were performed to figure out systematic trends hidden in the WK algorithms with respect to the reference method and are illustrated for  $P_f$  and  $P_b$  in Fig. 3. The mean reflection magnitude (RM) using the measured flow is 0.63 (0.10 SD), taking the triangular flow 0.56 (0.09 SD), using the averaged flow 0.72 (0.07 SD) and with the WK flow 0.59 (0.09 SD). For the reflection index (RI) the mean value using the measured flow is 0.38 (0.04 SD), taking the triangular flow 0.36 (0.04 SD), using the averaged flow 0.42 (0.02 SD) and with the WK flow 0.37 (0.04). For RM this results in a mean difference between WK and Doppler of  $-0.04$  (0.07 SD)  $[-0.052|-0.028]$  and  $-0.01$  (0.03 SD)  $[-0.015|-0.005]$  for RI, respectively. The mean RMSE for the separated curves using the measured flow and the triangular flow is 2.34 (1.57 SD), for the measured flow and the averaged flow 0.93 (0.41 SD) and between the measured flow and the WK flow 0.82 (0.54 SD). Please see Table 2 for summary.

### 3.4. Analysis of covariates

In stepwise regression analysis Doppler derived values of  $P_b$  were independently related to heart rate (HR), mean blood pressure (MBP) and age ( $R^2 = 0.35$ ,  $P < 0.001$ ). Weight, height and sex did not contribute significantly. The models for WK and average method showed similar results compared to Doppler providing no statistical significant differences for  $P_b$ . In the model for the triangular method also HR, MBP and age ( $R^2 = 0.35$ ,  $P < 0.001$ ) were independently related to  $P_b$ , however, the beta coefficients for HR and MBP significantly differed compared to Doppler and the other two models (always  $P < 0.01$ ).

Similar results could be obtained comparing the different models for  $P_f$ . Stepwise regression for forward pressure wave showed that MBP and age are independently related to  $P_f$  to the

**Table 3 – Stepwise regression analysis of deriving  $P_b$  and  $P_f$  by echo, WK, triangular and average method ( $P_f$  = forward pressure wave amplitude,  $P_b$  = backward pressure wave amplitude).**

Variables	$\beta$	SE ( $\beta$ )	P
Model for $P_b$ [mmHg] derived by echo, $R^2 = 0.35$ , $P < 0.001$			
HR	-0.10	0.04	<0.01
MBP	0.22	0.04	<0.001
Age	0.17	0.03	<0.001
Model for $P_b$ [mmHg] derived by WK, $R^2 = 0.34$ , $P < 0.001$			
HR	-0.08	0.04	<0.05
MBP	0.22	0.04	<0.001
Age	0.17	0.03	<0.001
Model for $P_b$ [mmHg] derived by triangular, $R^2 = 0.35$ , $P < 0.001$			
HR	-0.22	0.05	<0.001
MBP	0.33	0.05	<0.001
Age	0.16	0.04	<0.001
Model for $P_b$ [mmHg] derived by average, $R^2 = 0.35$ , $P < 0.001$			
HR	-0.09	0.04	<0.05
MBP	0.24	0.04	<0.001
Age	0.17	0.03	<0.001
Model for $P_f$ [mmHg] derived by echo, $R^2 = 0.22$ , $P < 0.001$			
HR	-0.02	0.06	<0.2*
MBP	0.25	0.06	<0.001
Age	0.20	0.05	<0.001
Model for $P_f$ [mmHg] derived by WK, $R^2 = 0.26$ , $P < 0.001$			
HR	-0.06	0.05	<0.2*
MBP	0.26	0.05	<0.001
Age	0.19	0.05	<0.001
Model for $P_f$ [mmHg] derived by triangular, $R^2 = 0.18$ , $P < 0.001$			
HR	-0.11	0.08	<0.1*
MBP	0.32	0.08	<0.001
Age	0.21	0.07	<0.01
Model for $P_f$ [mmHg] derived by average, $R^2 = 0.25$ , $P < 0.001$			
HR	-0.05	0.06	<0.2*
MBP	0.28	0.06	<0.001
Age	0.21	0.05	<0.001

\* Marks a non significant parameter.

same extent for Doppler, WK, average and triangular method derived values. Table 3 provides a full overview of the results.

Stepwise linear regression of the differences between AP and  $P_b$  derived by Doppler and WK showed similar results. HR, MBP and gender remained significant to the same extent in both models. Average method based differences were only related significantly to HR and gender. Residuals from triangular method showed only significance to gender. Table 4 provides a summary of the according numerical results.

## 4. Discussion

WSA parameters (amplitudes of forward and backward waves), obtained with the introduced Windkessel method (ARCSolver) and using non-invasively generated pressure waveforms, are similar compared to the reference method, which uses Doppler ultrasound derived flow waves and generated pressure waveforms. Analysis of covariates showed that these two methods can be used interchangeably in cohorts with preserved ejection fraction (EF). This may in future

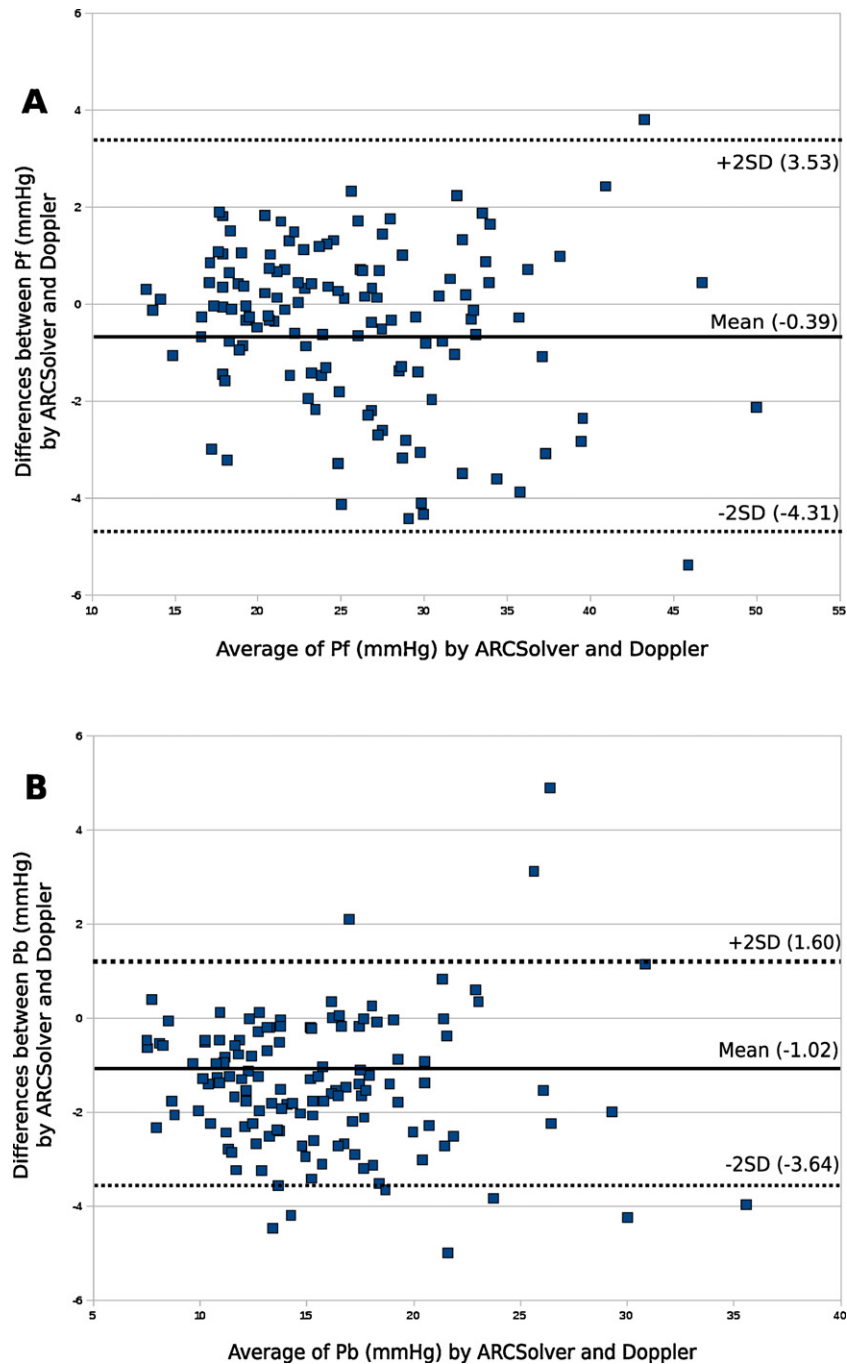


Fig. 3 – Bland–Altman plots of  $P_f$  (A) and  $P_b$  (B), respectively.

enable researchers and clinicians to acquire sophisticated blood-pressure related information easily and in a timely way.

The results for the estimated timing of the flow maximum ( $t_{Q_{max}}$ ) by the WK algorithms show good agreement with the reference method. The same outcome could be observed for the maximum slope of flow curve ( $dQ_{max}$ ). Both parameters are important determinants for accurate pulse wave decomposition. The RMSE and standard deviation of flow waveform compared to Doppler was lower for WK than for triangular flow.

Based on the derived flow waves the pressure waves were decomposed. Triangular flow modeling is reported to overestimate forward and backward pressure wave amplitudes compared to Doppler. In our data, as illustrated in Table 2, we could confirm this effect for triangular flow [22]. Kips et al. proposed an averaged flow waveform, which outperformed the triangulation. Windkessel flow also shows favorable results compared to triangular flow and provides similar accuracy compared to the averaged waveform from Kips et al.

Unlike the averaged flow waveform approach which indeed performs well, WK provides a functional framework, based on

**Table 4 – Stepwise regression analysis of differences between augmentation pressure (AP) and backward pressure wave amplitude ( $P_b$ ) derived by echo, WK, triangular and average method.**

Variables	$\beta$	SE ( $\beta$ )	P
Model for AP – $P_b$ [mmHg] derived by echo, $R^2 = 0.20$ , $P < 0.001$			
HR	–0.10	0.02	<0.001
MBP	0.07	0.02	<0.01
Age	0.02	0.02	>0.2*
Gender	2.21	0.62	<0.001
Model for AP – $P_b$ [mmHg] derived by WK, $R^2 = 0.24$ , $P < 0.001$			
HR	–0.13	0.02	<0.001
MBP	0.07	0.02	<0.01
Age	0.02	0.02	>0.2*
Gender	1.51	0.58	<0.05
Model for AP – $P_b$ [mmHg] derived by triangular, $R^2 = 0.07$ , $P < 0.05$			
HR	0.01	0.04	>0.2*
MBP	–0.04	0.04	>0.2*
Age	0.02	0.04	>0.2*
Gender	3.18	1.06	<0.01
Model for AP – $P_b$ [mmHg] derived by average, $R^2 = 0.15$ , $P < 0.001$			
HR	–0.10	0.03	<0.001
MBP	0.05	0.03	>0.2*
Age	0.02	0.03	>0.2*
Gender	2.13	0.73	<0.01

\* Marks a non significant parameter.

linear theory, which may allow in future the transformation of the presented findings to patients with impaired ejection fraction by adaption of mathematical constraints. Overall the results suggest that the methods are in good agreement without any systematic bias and that the WK method provides reduced variation compared to triangulation.

Beta-coefficients from stepwise regression analysis of covariates and determinants, derived from forward and backward wave amplitudes, showed no significant difference between WK and reference (Doppler-based) method, suggesting similar physiological meaning of the parameters derived with the respective methods. These findings could not be confirmed for average and triangular method. Noteworthy and similar to results obtained with the reference (Doppler-based) method in a large population study [30], only the amplitudes of the forward and the backward waves derived from the WK method reflect the influence of HR, MBP, age and gender adequately. This may represent one of the most important differences to the pulse waveform analysis-based AP.

Nevertheless our study has certain limitations: The digitalization of the measured velocity profiles is carried out manually, therefore a certain amount of subjectivity cannot be excluded. The averaged flow curve developed by Kips and co-workers is based on a younger cohort than the one used for this study. An averaged flow curve derived from age matched patients might perform better than the curve published by Kips et al. used here. The aortic pulse wave shape used here is gained via a generalized transfer function from a peripheral recording. Such a reconstructed pressure curve may miss characteristics important for wave separation [5]. WSA in this study is based on information gained from the reconstructed pressure wave, which may introduce a systematic bias.

Therefore the unavailability of invasive recordings needs to be acknowledged as a limitation.

## 5. Perspectives

The results of this study indicate that the measurements for WSA parameters agree with the reference method for the proposed algorithm in a population with preserved ejection fraction. The functional nature of the introduced approach may allow to transfer the actual findings to cohorts with impaired ejection fraction in future. This shall widen the future opportunities to study sophisticated arterial hemodynamics in larger cross-sectional studies, in trials of drug effects, and in longitudinal studies.

## Conflicts of interest

S.W. and C.M. are inventors of a patent which is partly used in ARCSolver. The other authors report no conflicts of interest.

## Sources of funding

This work and its publication was partly supported by a grant of the Government of Lower Austria and the EC (EFRE), contract number WST3-T-81/015-2008.

## Appendix A.

### A.1. Waveform construction

The ARCSolver describes the outflow of the left ventricle based on an externally provided central pressure waveform by the means of a dynamic system using a second order ordinary differential equation.

During systole the relation between pressure ( $p(t)$ ), aortic root flow ( $q(t)$ ) and peripheral aortic flow ( $x(t)$ ) can be described as in ApEqs. (1) and (2).

$$q(t) = R_p \times C_a \times x'(t) + x(t) \quad \text{for } 0 < t < t_s \quad (1)$$

$$p(t) = R_c \times q(t) + R_p \times x(t) \quad (2)$$

Here  $R_p$  is the peripheral resistance,  $R_c$  is the effective arterial resistance and  $C_a$  is the arterial compliance. The first derivative of the flow in the aorta with respect to time is denoted as  $x'(t)$ , the end of the ejection time is marked as  $t_s$ . When the aortic valve is closed, the outflow is modeled to be zero, which is an obvious assumption, resulting in an mono exponential decay for  $x(t)$  in diastole; see ApEqs. (3) and (4), where  $t_d$  denotes the end of diastole, which is synonymous with the end of the cardiac cycle.

$$q(t) = 0 \quad \text{for } t_s \leq t \leq t_d \quad (3)$$

$$x(t) = x(0) \times e^{t_d - t / R_p C_a} \quad (4)$$

The initial value in ApEq. (4) is specified in the way that periodicity of the signal is guaranteed:

$$x(0) = x(t_d) \tag{5}$$

The work of the heart over one cardiac cycle can now be calculated as:

$$W = \int_0^{t_s} p(t) \times q(t) dt \tag{6}$$

The aim is to minimize this integral (ApEq. (6)) under the constraint that a certain stroke volume has to be reached:

$$\int_0^{t_s} q(t) dt = V_s \tag{7}$$

Furthermore the following physiological boundary conditions should be fulfilled (see ApEq. (3)):

$$q(0) = 0 \tag{8}$$

$$q(t_s) = 0 \tag{9}$$

This problem can be solved using the calculus of variations. Substituting  $p(t)$  and  $q(t)$  in ApEq. (6) using ApEqs. (1) and (2), the integrand can be written as a function  $F = F(x, x', t)$ . The isoperimetric constraint in ApEq. (7) can be incorporated to  $F$  using a Lagrange multiplier  $\mu$ . Hence  $F$  can be written as:

$$F(x, x', t, \mu) = (R_c + R_p) \times x^2 + (2 \times R_p \times C_a \times R_c + R_p^2 \times C_a) \times x \times x' + R_p^2 \times C_a^2 \times R_c \times x'^2 - \mu \times (R_p \times C_a x' + x) \tag{10}$$

The solution for such a problem can be determined by the solution of the Euler-Lagrange-equation:

$$\frac{\partial F}{\partial x} - \frac{d}{dt} \frac{\partial F}{\partial x'} = 0 \tag{11}$$

The partial derivatives involved in the equation can be calculated as:

$$\frac{\partial F}{\partial x} = 2(R_c + R_p)x + (2R_p C_a R_c + R_p^2 C_a)x' - \mu \tag{12}$$

$$\frac{\partial F}{\partial x'} = (2R_p C_a R_c + R_p^2 C_a)x + 2R_p^2 C_a^2 R_c x' - \mu R_p C_a \tag{13}$$

$$\frac{d}{dt} \frac{\partial F}{\partial x'} = (2R_p C_a R_c + R_p^2 C_a)x' + 2R_p^2 C_a^2 R_c x'' \tag{14}$$

Since  $F$  contains a first derivative of  $x(t)$  and the Euler-Lagrange equation includes a derivation with respect to time, the result is always an inhomogeneous linear second order ordinary differential equation, see ApEq. (15). The inhomogeneity results of course from the constraint incorporated in  $F$ .

$$x'' - \alpha^2 \times x = \beta \tag{15}$$

The coefficients  $\alpha$  and  $\beta$  are time-invariant but depend on several model parameters:  $\alpha = \alpha(R_c, R_p, C_a)$  and  $\beta = \beta(R_c, R_p, C_a, \mu)$ .

Following the theory of ordinary differential equations, the solution has the following form:

$$x(t) = A \times e^{\alpha \times t} + B \times e^{-\alpha \times t} + C \tag{16}$$

Inserting the general solution of the differential equation ApEq. (16) to ApEqs. (4), (7) and (9) yields to a system of three linear equations and therefore solutions for  $A, B$  and  $C$  that can be found uniquely. Since  $V_s$  is unknown, it has to be approximated by:

$$V_s = \frac{p_{\text{mean}}}{R_p} t_d \tag{17}$$

The parameters  $R_p, R_c$  and  $C_a$  are now varied over a certain physiological range to find their optimal values to fit the given pressure waveform. As optimization criteria the area under the pressure curve is used.

As described above the proposed solution of the differential equation consists of three unknown parameters that have to be determined. But with ApEq. (4) and ApEqs. (7)–(9) four boundary conditions were formulated. Therefore one constraint has to be omitted, and ApEq. (8) has been left out. The disadvantage of this kind of approach is that the resulting flow curve (Fig. 2B) does reflect the right area of the flow curve but not reflect the real flow waveform due to the neglected initial condition ApEq. (8), which would inhibit its use for the wave separation analysis. Therefore in an additional step the initially calculated left ventricular outflow (Fig. 2B) is processed using a discrete linear second order delay element (ApEq. (18)) for further reshape.

$$\begin{pmatrix} b_{t+1} \\ Q_{t+1} \end{pmatrix} = \begin{pmatrix} 1 - \frac{1}{T_1} & 0 \\ \frac{1}{T_2} & 1 - \frac{1}{T_2} \end{pmatrix} \cdot \begin{pmatrix} b_t \\ Q_t \end{pmatrix} + \begin{pmatrix} \frac{1}{T_1} \cdot q_t \\ 0 \end{pmatrix} \tag{18}$$

Here the initial conditions are set to be zero ( $b_0 = 0, Q_0 = 0$ ). The time constants ( $T_1$ ) and ( $T_2$ ) of the delay depend on the slope of the pressure curve in early systole and naturally on the underlying time step. While  $T_1$  is hold constant over time,  $T_2$  is a time-dependent parameter decreasing linearly from  $T_1$  to one, influencing the reshape of the flow curve mainly during systolic upstroke.  $b$  is an intermediate state variable and  $Q$  denotes the flow curve used for further processing in the wave separation analysis, illustrated in Fig. 2C. Once more during diastole the flow is assumed to be zero.

### A.2. Wave separation analysis

To perform the separation, three variables are needed: The pressure and flow wave in the aorta and furthermore the characteristic impedance ( $Z_c$ ), which represents the impact of the arterial wall.  $Z_c$  is estimated in the frequency domain using the modulus of the complex input impedance ( $Z$ ) (ApEq. (19)), calculated from the ratio of the present pressure and flow in the frequency domain.

$$\frac{P_m}{Q_m} = Z \tag{19}$$

The frequencies in the range of 4–10 Hz are taken into account, which is a commonly used procedure. For higher frequencies there could be inaccuracy due to noise. To minimize the influence of outliers, all input impedances greater than a factor of 3 of the median of the considered impedances, are not taken into account. Following the wave theory, the measurable pressure ( $P_m$ ) in the aorta is the sum of forward ( $P_f$ ) and backward ( $P_b$ ) traveling waves.

$$P_m = P_f + P_b \quad (20)$$

The same is valid for the corresponding flow waves.

$$Q_m = Q_f + Q_b \quad (21)$$

Subsequently the relationship between pressure and flow can be described as

$$P_f = Z_c \times Q_f \quad (22)$$

$$P_b = -Z_c \times Q_b \quad (23)$$

So far it is only possible to measure the sum of the forward and backward going waves. To obtain the forward and backward going parts separately, these equations have to be transformed, in order to obtain explicit formulas for the requested parameters.

$$P_f = 0.5 \times (P_m + Z_c \times Q_m) \quad (24)$$

$$P_b = 0.5 \times (P_m - Z_c \times Q_m) \quad (25)$$

It should be noted that the absolute amplitude of  $Q_m$  is not relevant for the decomposition. If  $Q_m$  is changed by a certain factor, the resulting characteristic impedance will be altered by the same factor in an inverse manner. Thus the calculated waves in forward and backward direction remain unchanged.

Based on these amplitudes, two parameters can be derived, the reflection magnitude (RM) and the reflection index (RI). The reflection magnitude is the quotient of the backward and forward amplitude of the separated pressure waves.

$$RM = \frac{\max(P_b) - \min(P_b)}{\max(P_f) - \min(P_f)} \quad (26)$$

For the reflection index the denominator is changed to the sum of the two amplitudes.

$$RI = \frac{\max(P_b) - \min(P_b)}{\max(P_f) - \min(P_f) + \max(P_b) - \min(P_b)} \quad (27)$$

## REFERENCES

- [1] E. Agabiti-Rosei, G. Mancia, M.F. O'Rourke, M.J. Roman, M.E. Safar, H. Smulyan, J.G. Wang, I.B. Wilkinson, B. Williams, C. Vlachopoulos, Central blood pressure measurements and antihypertensive therapy: a consensus document, *Hypertension* 50 (2007) 154–160.
- [2] A. Avolio, L.M. Van Bortel, P. Boutouyrie, J.R. Cockcroft, C.M. McEnery, A.D. Protogerou, M.J. Roman, M.E. Safar, P. Segers, H. Smulyan, Role of pulse pressure amplification in arterial hypertension, *Hypertension* 54 (2009) 375–383.
- [3] G. Mancia, G. De Backer, A. Dominiczak, R. Cifkova, R. Fagard, G. Germano, G. Grassi, et al., Guidelines for the management of arterial hypertension, *European Heart Journal* 28 (2007) 1462–1536.
- [4] L.M. Van Bortel, D. Duprez, M.J. Starmans-Kool, M.E. Safar, C. Giannattasio, J. Cockcroft, D.R. Kaiser, C. Thuillez, Clinical applications of arterial stiffness, task force. III: Recommendations for user procedures, *American Journal of Hypertension* 15 (2002) 445–452.
- [5] C. Chen, E. Nevo, B. Fetits, P. Pak, F. Yin, W.L. Maughan, D. Kass, Estimation of central aortic pressure waveform by mathematical transformation of radial tonometry pressure: validation of generalised transfer function, *Circulation* 95 (1997) 1827–1836.
- [6] R. Kelly, C. Hayward, A. Avolio, M. O'Rourke, Noninvasive determination of age-related changes in the human arterial pulse, *Circulation* 80 (1989) 1652–1659.
- [7] J. Nürnberger, A. Keflioglu-Scheiber, A.O. Saez, R.R. Wenzel, T. Philipp, R.F. Schäfers, Augmentation index is associated with cardiovascular risk, *Journal of Hypertension* 20 (2002) 2407–2414.
- [8] G.M. London, J. Blacher, B. Pannier, A.P. Guerin, S.J. Marchais, M.E. Safar, Arterial wave reflections and survival in end-stage renal failure, *Hypertension* 38 (2001) 434–438.
- [9] M.E. Safar, J. Blacher, B. Pannier, A.P. Guerin, S.J. Marchais, P.M. Guyonvarch, G.M. London, Central Pulse pressure and mortality in end-stage renal disease, *Hypertension* 39 (2002) 735–738.
- [10] P. Jankowski, K. Kawecka-Jaszcz, D. Czarnecka, M. Brzozowska-Kiszka, K. Styczkiewicz, M. Loster, M. Kloch-Badelek, J. Wilinski, A. Curylo, D. Dudek, Pulsatile but not steady component of blood pressure predicts cardiovascular events in coronary patients, *Hypertension* 51 (2008) 1–8.
- [11] T. Nishijima, Y. Nakayama, K. Tsumura, N. Yamashita, K. Yoshimaru, H. Ueda, et al., Pulsatility of ascending aortic blood pressure waveform is associated with an increased risk of coronary heart disease, *American Journal of Hypertension* 14 (2001) 469–473.
- [12] T. Weber, J. Auer, M.F. O'Rourke, E. Kvas, E. Lassnig, R. Berent, B. Eber, Arterial stiffness, wave reflections, and the risk of coronary artery disease, *Circulation* 109 (2004) 184–189.
- [13] T. Weber, M.F. O'Rourke, E. Lassnig, M. Prodoko, M. Ammer, M. Rammer, B. Eber, Pulse waveform characteristics predict cardiovascular events and mortality in patients undergoing coronary angiography, *Journal of Hypertension* 28 (2010) 797–805.
- [14] S.J. Marchais, A.P. Guerin, B.M. Pannier, B.I. Levy, M.E. Safar, G.M. London, Wave reflections and cardiac hypertrophy in chronic uremia. Influence of body size, *Hypertension* 22 (1993) 876–883.
- [15] M.J. Roman, R.B. Devereux, J.R. Kizer, E.T. Lee, J.M. Galloway, T. Ali, J.G. Umans, B.V. Howard, Central pressure more strongly relates to vascular disease and outcome than does brachial pressure: the strong heart study, *Hypertension* 50 (2007) 197–203.
- [16] M.F. O'Rourke, M.G. Taylor, Input impedance of the systemic circulation, *Circulation Research* 20 (1967) 365–380.
- [17] C.J. Mills, I.T. Gabe, J.H. Gault, D.T. Mason, J. Ross, E. Braunwald, J.P. Shillingford, Pressure–flow relationships and vascular impedance in man, *Cardiovascular Research* 4 (1970) 405–417.

- [18] N. Westerhof, P. Sipkema, G.C. van den Bos, G. Elzinga, Forward and backward waves in the arterial system, *Cardiovascular Research* 6 (1972) 648–656.
- [19] J.P. Murgo, N. Westerhof, J.P. Giolma, S.A. Altobelli, Aortic input impedance in normal man: relationship to pressure wave forms, *Circulation* 62 (1980) 105–116.
- [20] J.P. Murgo, B.R. Alter, J.F. Dorethy, S.A. Altobelli, G.M. McGranahan, Dynamics of left ventricular ejection in obstructive and nonobstructive hypertrophic cardiomyopathy, *Journal of Clinical Investigation* 66 (1980) 1369–1382.
- [21] W.W. Nichols, M.F. O'Rourke, C. Vlachopoulos, McDonald's *Blood Flow in Arteries*, 6th ed., Arnold, London, 2011.
- [22] J.G. Kips, E.R. Rietzschel, M.L. De Buyzere, B.E. Westerhof, T.C. Gillebert, L.M. van Bortel, P. Segers, Evaluation of noninvasive methods to assess wave reflection and pulse transit time from the pressure waveform alone, *Hypertension* 53 (2009) 142–147.
- [23] A. Qasem, A. Avolio, Determination of aortic pulse wave velocity from waveform decomposition of the central aortic pressure pulse, *Hypertension* 51 (2008) 188–195.
- [24] B.E. Westerhof, I. Guelen, N. Westerhof, J.M. Karemaker, A. Avolio, Quantification of wave reflection in the human aorta from pressure alone: a proof of principle, *Hypertension* 48 (2006) 595–601.
- [25] K.H. Wesseling, J.R.C. Jansen, J.J. Settles, J.J. Schreuder, Computation of aortic flow from pressure in humans using a nonlinear, three-element model, *Journal of Applied Physiology* 74 (1993) 2566–2573.
- [26] S.C.A.T. Davis, B.E. Westerhof, B. van den Bogaard, L.W.J. Bogert, J. Truijten, Y.S. Kim, N. Westerhof, J.J. van Lieshout, Active standing reduces wave reflection in the presence of increased peripheral resistance in young and old healthy individuals, *Journal of Hypertension* 29 (2011) 682–689.
- [27] A. Avolio, G. Parati, Reflecting on posture, *Journal of Hypertension* 29 (2011) 655–657.
- [28] K.L. Wang, H.M. Cheng, S.H. Sung, S.Y. Chuang, C.H. Li, H.A. Spurgeon, C.T. Ting, S.S. Najjar, E.G. Lakatta, F.C.P. Yin, P. Chou, C.H. Chen, Wave reflection and arterial stiffness in the prediction of 15-year all-cause and cardiovascular mortalities. A community-based study, *Hypertension* 55 (2010) 799–805.
- [29] T. Weber, S. Wassertheurer, M. Rammer, A. Haiden, B. Hametner, B. Eber, Wave reflections, assessed with a novel method for pulse wave separation, are associated with end-organ damage and clinical outcomes, *Hypertension* 60 (2012) 534–541.
- [30] P. Segers, E.R. Rietzschel, M.L. De Buyzere, S.J. Vermeersch, D. De Bacquer, L.M. van Bortel, J. DeBacker, T.C. Gillebert, P.R. Verdonck, Noninvasive (input) impedance, pulse wave velocity, and wave reflection in healthy middle-aged men and women, *Hypertension* 49 (2007) 1248–1255.
- [31] N. Stergiopoulos, P. Segers, N. Westerhof, Use of pulse pressure method for estimating total arterial compliance in vivo, *American Journal of Physiology. Heart and Circulatory Physiology* 276 (1999) H424–H428.
- [32] R.P. Hämmäläinen, J.J. Hämmäläinen, On the minimum work criterion in optimal control models of left-ventricular ejection, *IEEE Transactions on Biomedical Engineering* 32 (1985) 951–956.
- [33] S. Wassertheurer, J. Kropf, T. Weber, M. van der Giet, J. Baulmann, A. Ammer, B. Hametner, C.C. Mayer, B. Eber, D. Magometschnigg, A new oscillometric method for pulse wave analysis: comparison with a common tonometric method, *Journal of Human Hypertension* 24 (2010) 498–504.
- [34] S. Wassertheurer, C. Mayer, F. Breiteneker, Modeling arterial and left ventricular coupling for non-invasive measurements, *Simulation Modelling Practice and Theory* 16 (2008) 988–997.
- [35] S.M. Yamashiro, J.A. Daubenspeck, F.M. Bennett, Optimal regulation of left ventricular ejection pattern, *Applied Mathematics and Computation* 5 (1979) 41–54.
- [36] A. Swillens, P. Segers, Assessment of arterial pressure wave reflection: methodological considerations, *Artery Research* 2 (2008) 122–131.